

Conformational transition in DNA on a cold surface

X. Z. Feng, R. Bash¹, P. Balagurumoorthy², D. Lohr¹, R. E. Harrington² and S. M. Lindsay*

Department of Physics and Astronomy, ¹Department of Chemistry and Biochemistry and ²Department of Microbiology, Arizona State University, Tempe, AZ 85287-1504, USA

Received August 23, 1999; Revised and Accepted November 5, 1999

ABSTRACT

The contour length of DNA fragments, deposited and imaged on mica under buffer, was measured as a function of deposition temperature. Extended DNA molecules (on Ni- and silane-treated surfaces) contract rapidly with falling temperature, approaching the contour length of A-DNA at 2°C. The contraction is not unique to a specific sequence and does not occur in solution at 2°C or on a surface at 25°C, indicating that it arises from a combination of low temperature and surface contact. It is probably a consequence of reduced water activity at a cold surface.

INTRODUCTION

DNA is a conformationally labile molecule that exists in a variety of structural forms depending upon its ionic environment, the local water activity and its base sequence (1). High resolution electron (2) or atomic force (3,4) microscopy offers one way to explore this behavior. Atomic force microscopy (AFM) permits samples to be deposited and imaged in buffer, but it still requires attachment of the molecules to a surface. Important properties of a liquid, such as ionic strength, are altered near a surface (5) and the surface itself excludes water so that conformational transitions might be induced by the act of attaching a molecule to a surface, even under a physiological buffer.

Rivetti *et al.* (6,7) have studied the change in chain statistics that occurs as a molecule becomes trapped at a solid–liquid interface, while Fang *et al.* showed how DNA dried onto mica after deposition from ethanol/water mixtures (8) exists in a mixture of B- and A-forms. There has not, as yet, been a clear demonstration of an internal conformational transition induced by surface effects alone. In this paper, we show that DNA adsorbed onto a cold surface undergoes a transition to an A-like form, while identical DNA in solution shows no sign of a conformational change in its circular dichroism. The observation is of some interest beyond the field of microscopy because a classic way of studying DNA bending utilizes low temperature gel mobility (9) and because the genome of organisms that live in extremely cold environments is in contact with a cold, condensed medium (10).

MATERIALS AND METHODS

DNA samples

We used a 907 bp yeast fragment containing the *GALI-10* intergenic region (11) and a 603 bp fragment from a *HaeIII*

digest of ϕ x174 as a control sample of different sequence. Both samples were passed twice through a NAP-10 column (Pharmacia) equilibrated with freshly distilled water. The DNA solution was dried in a Speed Vac (Savant) and redissolved in 0.1 mM Tris–HCl, pH 8.00. From this stock solution, DNA was diluted to a concentration of 2 ng/ μ l with 0.1 mM Tris–HCl, pH 8.00, and then deposited for imaging. Solutions for DNA imaging were made with 18 M Ω water from a Nanopure system (Barnstead, Dubuque, IA) that had been redistilled with KMNO₄ to remove organic debris from the filters.

Mica activation and sample deposition

AP-mica. 3-Aminopropyltriethoxysilane (APTES) (98%; Sigma Chemical Co., St Louis, MO) was distilled once under vacuum prior to use. Mica was treated with this reagent (AP-mica) by suspending one part APTES in 1000 parts water, placing 100 μ l of this suspension on freshly cleaved mica and leaving it for 5 min. The surface was rinsed with 200 μ l of clean water and blown dry with clean argon gas. An aliquot of 300 μ l of DNA solution (2 ng/ μ l in 0.1 mM Tris–HCl, pH 8) was placed on the mica in the AFM liquid cell and imaged after 10 min. We have found this method to be more reliable than the earlier vapor-based technique (12–14). For deposition below 25°C, the mica was prepared as described above and, after drying, mounted on the sample plate of the AFM (see below) and then placed in an enclosure submerged in a thermostatted water bath in a cold room (1.8°C). The stock solutions were placed in the same water bath and temperature equilibration was monitored by means of a thermocouple attached to the stainless steel sample plate of the AFM. Spatial uniformity of the sample temperature was checked by monitoring multiple points. Equilibration at the lowest temperatures took ~20 min. The sample was deposited onto the mica quickly inside the enclosure and incubated for 10 min. The sample plate was allowed to come back to room temperature (20 min) and then placed in the microscope for imaging.

Mg-mica. Magnesium-treated mica was prepared by placing 100 μ l of 4 mM MgCl₂ onto freshly cleaved mica and incubating for 5 min. It was subsequently washed and treated with DNA in Tris–HCl as described above with no additional Mg in the buffer.

Ni-mica. Nickel-treated mica was prepared using 100 μ l of 100 mM NiCl₂ solution incubated for 5 min and then washed. All subsequent treatments were as described above.

*To whom correspondence should be addressed. Tel: +1 480 965 4691; Fax: +1 480 965 7954; Email: stuart.lindsay@asu.edu

AFM imaging

We used a PicoSPM from Molecular Imaging (Phoenix, AZ). This instrument utilizes a top-down scanner with a lightweight sample plate suspended below it magnetically. The liquid cell is a one piece Teflon well which clips onto the mica on the sample plate, facilitating sample exchange and temperature control. Images were taken with a magnetic AC drive (MacMode) using silicon MacLevers of nominal spring constant 0.6 N/m. The free operating amplitude was set at 5 nm p/p with a 10% reduction set point. The drive frequency was 25 kHz. Images were saved in tif format and analyzed using NIH Image. Contour length was measured by tracing the molecular contour with a segmented line. End-to-end length was measured from the shortest straight line that connected the ends of an image.

The instrument was calibrated at regular intervals using a 1 μm square grating (Silicon MDT, Moscow), checked by measuring the contour length of pUC19 plasmids. Absolute calibration was somewhat better than 1% but random errors in following contours on imperfect images raise the overall uncertainty to ~3%.

CD spectroscopy

The 907 bp fragment was purified as described above and dissolved to a final concentration of 50 $\mu\text{g/ml}$ in 0.1 mM Tris-HCl, pH 8.00. Spectroscopy was carried out in a thermostatted 1 cm path length cell using a Jasco model J-710 CD spectrophotometer. Temperature was monitored using a thermocouple placed in the cuvette near the light path.

RESULTS AND DISCUSSION

Several different approaches to binding DNA for imaging under buffer have been described in the literature (14–18). The precise nature of the DNA–surface interactions is still unclear so we set out to compare three different methods: (i) AP-mica (14); (ii) nickel-treated mica (15); and (iii) mica treated with Mg alone (18) without the use of HEPES (17). We found that the magnesium treatment causes linear DNA to condense on the surface (an effect not observed with small circles; 18). Although these condensed features were temperature dependent, we chose only to analyze images from the Ni- and AP-mica because they showed some DNA molecules that were extended enough to measure a contour length. At lower temperatures, many of the molecules appeared to condense, limiting the number of molecules from which accurate length data were obtained.

Comparative images of DNA deposited and imaged in buffer on Ni- and AP-mica are shown in Figure 1 for depositions at 25 and 1.8°C. Contrast and resolution varied considerably from run to run and the images shown were selected to be of comparable scan size. For the AP-mica, we found that the density of features, both extended chains and condensed ‘blobs’, increased markedly at lower temperatures. Results with Ni-treated mica were similar, but yielded somewhat lower resolution (Fig. 1c and d).

We did not image at low temperatures, but we did monitor the samples over periods varying from 10 min after deposition to several days, seeing no measurable changes in the images. The changes in length between the warmest (25°C) and coldest

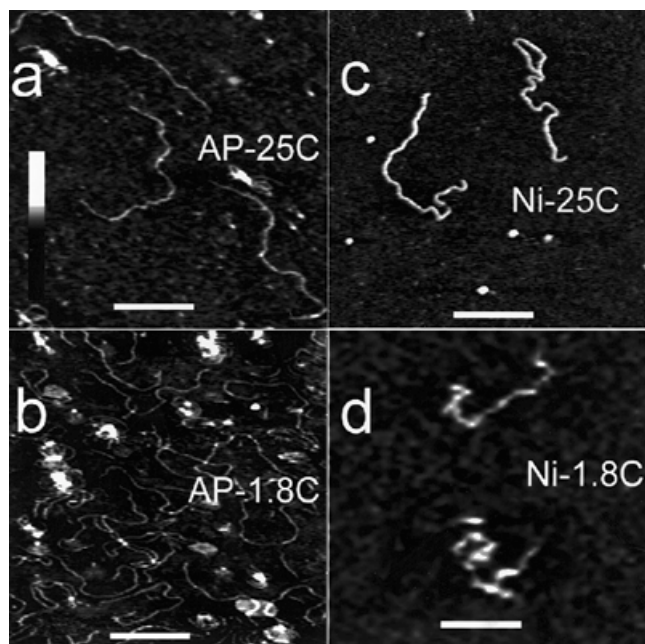


Figure 1. AFM images of DNA on mica surfaces treated with APTES (a and b) or Ni (c and d). The upper panels (a and c) were for DNA deposited at 25°C and the lower panels (b and d) were for DNA deposited at 1.8°C. Scale bars are all 100 nm. The height scale for all images is 0–8 nm and is shown on the left of (a). Images were processed by flattening and contrast adjustment.

(1.8°C) deposition temperatures were reproduced in several experiments, showing that if there are changes on warming the sample after deposition, the state of the sample nonetheless reflects the deposition temperature.

The contour length and end-to-end length measured for several 907 bp molecules on AP-mica as a function of deposition temperature are summarized in Table 1. DNA bending is known to be enhanced in solution as the temperature is lowered (9). The significant decrease of the end-to-end length (Table 1) shows that this is also true for the population of molecules that are adsorbed onto the mica surface.

More striking, however, is the dramatic decrease in contour length as temperature is lowered. The rise per base falls from 0.35 ± 0.01 nm, corresponding to the B-DNA rise, to 0.27 ± 0.01 nm, corresponding to the A-DNA rise (1), at the coldest temperature. This result suggests that we are observing a B- to A-DNA transition. We note that most of the bending enhancement occurs by 10°C whereas the B to A transition occurs below this temperature.

Contour length measurements are summarized graphically in terms of rise per base in Figure 2, where the upper line corresponds to the B-DNA rise per base and the lower line to the same quantity for A-DNA. All error bars show ± 1 SD. Crosses are data for the 907 bp fragment on AP-mica and dots are for the same DNA on Ni-mica. Data for the 603 bp fragment on AP-mica are shown as triangles. These results demonstrate that the effect is (i) independent of the specific surface treatment (AP- or Ni-mica) and (ii) independent of the particular sequence of the DNA (although we have not explored the effects of large changes in GC content).

Table 1. End-to-end and contour length measurements for the 907 bp DNA on AP-mica as a function of temperature

Temperature (°C)	End-to-end length (nm)	Contour length (nm)	Number of molecules
25.0	173 ± 47	319 ± 13	26
19.1	167 ± 69	314 ± 8	5
12.0	129 ± 30	303 ± 12	8
10.0	97 ± 44	319 ± 7	7
9.4	118 ± 38	295 ± 9	7
5.8	78 ± 22	278 ± 13	5
2.6	95 ± 53	265 ± 21	6
1.8	85 ± 43	246 ± 10	15

Errors are ±1 SD.

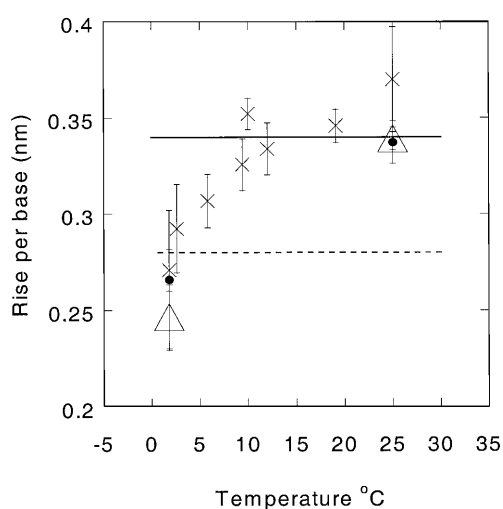


Figure 2. Rise per base as a function of temperature for 907 bp DNA on AP-mica (crosses), 907 bp DNA on Ni-mica (dots) and 603 bp DNA on AP-mica (triangles). The upper line shows the B-DNA rise per base and the lower line shows the same quantity for A-DNA. Error bars are ±1 SD.

It is quite reasonable to expect that a surface might induce a B to A transition. Although the mica surface is nominally hydrophilic, hydrocarbon adsorption on preparation will change its nature considerably (19). Those parts of the DNA in contact with the surface will be less hydrated than they would be in solution. The ionic strength of the solution will also be much higher close to the surface, depending upon the specific charge of the surface. For unmodified mica in pH 7 solution, this charge is $\sim 0.003 \text{ C/m}^2$ (20), corresponding to $\sim 1 \text{ M}$ ion concentration at the surface (5). Hydration effects are entropy driven, so the effect of the relative hydrophobicity of the surface environment will be enhanced at lower temperature, increasing the driving force for a B to A transition (21).

The twist of DNA in solution changes by about $-0.2^\circ \times 10^{-2}$ per $^\circ\text{C}$ (22,23), or $\sim 40^\circ$ for the 907 bp fragment over the full temperature range. If we assume that this small twist may be translated into a linear contraction of 10 bp per full turn (obviously an overestimate), this would produce a length change of $<0.1\%$. This cannot account for the dramatic changes observed

in this work. B to A transitions have been reported under some unusual solution conditions on cooling (24,25), so we checked the CD spectra of the 907 bp DNA to see if it underwent the B to A transition in solution. Results of measurements made at 30, 14 and 2°C essentially overlap one another (data not shown), showing that the transition we observe in the AFM data does not occur in solution. Thus, it is linked to the presence of a surface and is driven by lowering temperature.

We also studied the supercoiled plasmid pUC19, but found that almost all of the DNA collapsed on cooling into a form that did not permit measurement of contour lengths. Interestingly, some of the small minority that did not collapse did not appear to change length when cold.

CONCLUSIONS

We have shown that a cold surface can drive a B to A transition in DNA that would be in the B-form in solution at this temperature. This occurs even though the sample is deposited and imaged entirely under buffer. This clearly demonstrates the ability of the surface to change the structure of DNA in addition to its well-known effect on the polymer chain statistics (6,7). The influence of surface binding is clearly the major experimental issue confronting microscopy at the molecular level, and one that AFM is ideally suited to investigate, given the simplicity of sample preparation and the ability to image *in situ*.

ACKNOWLEDGEMENTS

We thank Judy Zhu of Molecular Imaging for telling us about her techniques for preparing AP-mica, Dan Brune for assistance with CD measurements and P.S. Ho for useful discussions. This work was supported, in part, by grants CA70274 and GM53517 from the NIH and DBI9513233 from the NSF.

REFERENCES

1. Saenger, W. (1984) *Principles of Nucleic Acid Structure*. Springer, New York, NY.
2. Griffith, J.D., Lee, S. and Wang, Y.H. (1997) *Curr. Opin. Struct. Biol.*, **7**, 362–366.
3. Hansma, H.G. and Hoh, J. (1994) *Annu. Rev. Biophys. Biomol. Struct.*, **23**, 115–139.

4. Bustamante, C., Rivetti, C. and Keller, D.J. (1997) *Curr. Opin. Struct. Biol.*, **7**, 709–716.
5. Israelachvili, J.N. (1991) *Intermolecular and Surface Forces*, 2nd Edn. Academic Press, New York, NY.
6. Rivetti, C., Walker, C. and Bustamante, C. (1998) *J. Mol. Biol.*, **280**, 41–59.
7. Rivetti, C., Guthold, M. and Bustamante, C. (1996) *J. Mol. Biol.*, **264**, 919–932.
8. Fang, Y., Spisz, T.S. and Hoh, J.H. (1999) *Nucleic Acids Res.*, **27**, 1943–1949.
9. Schroth, G.P., Siino, J.A., Cooney, C.A., Th'ng, P.H., Shing Ho, P. and Bradbury, E.M. (1992) *J. Biol. Chem.*, **267**, 9958–9964.
10. Priscu, J.C., Fritsen, C.H., Adams, E.E., Giovannoni, S.J., Paerl, H.W., Doran, P.T., Gordon, D.A., Lanoil, B.D. and Pinckey, J.L. (1998) *Science*, **289**, 2095–2098.
11. St John, T. and Davis, R. (1979) *Cell*, **16**, 443–452.
12. Lindsay, S.M., Lyubchenko, Y.L., Gall, A.A., Shlyakhtenko, L. and Harrington, R.E. (1992) *SPIE Proc.*, **1639**, 84–90.
13. Lyubchenko, Y.L., Oden, P.I., Lampner, D., Lindsay, S.M. and Dunker, K.A. (1993) *Nucleic Acids Res.*, **21**, 1117–1123.
14. Lyubchenko, Y.L., Shlyakhtenko, L., Harrington, R.E., Oden, P.I. and Lindsay, S.M. (1993) *Proc. Natl Acad. Sci. USA*, **90**, 2137–2140.
15. Hansma, H.G. and Laney, D.E. (1996) *Biophys. J.*, **70**, 1933–1939.
16. Thomson, N.H., Kasas, S., Smith, B., Hansma, P.K. and Hansma, H.G. (1996) *Langmuir*, **12**, 5905–5908.
17. Zuccheri, G., Dame, R.T., Aquila, M. and Samori, B. (1998) *Appl. Phys.*, **A66**, S585–S589.
18. Han, W., Dlakic, M., Harrington, R.E., Zhu, J. and Lindsay, S.M. (1997) *Proc. Natl Acad. Sci. USA*, **94**, 10565–10570.
19. Smith, T. (1980) *J. Colloid Interface Sci.*, **75**, 51–53.
20. Muller, D.J., Amrein, M. and Engel, A. (1997) *J. Struct. Biol.*, **119**, 172–188.
21. Basham, B., Schroth, G.P. and Ho, P.S. (1995) *Proc. Natl Acad. Sci. USA*, **92**, 6464–6468.
22. Pulleyblank, D.E., Shure, M., Tang, D., Vinograd, J. and Vosberg, H.-P. (1975) *Proc. Natl Acad. Sci. USA*, **72**, 4280–4284.
23. Depew, R.E. and Wang, J.C. (1975) *Proc. Natl Acad. Sci. USA*, **72**, 4275–4279.
24. Minchenkova, L.E., Schyolkina, A.K., Chernov, B.K. and Ivanov, V.I. (1986) *J. Biomol. Struct. Dyn.*, **4**, 463–476.
25. Kumar, G.S. and Maiti, M. (1994) *J. Biomol. Struct. Dyn.*, **12**, 183–200.